

Progress in understanding magnetic reconnection in laboratory and space astrophysical plasmas^{a)}

Masaaki Yamada^{b)}

Center of Magnetic Self-organization in Laboratory and Astrophysical Plasmas, Princeton Plasma Physics Laboratory, Princeton University, Princeton, New Jersey 08543-0451

(Received 2 November 2006; accepted 28 February 2007; published online 24 May 2007; publisher error corrected 30 May 2007)

This paper reviews the progress in understanding the fundamental physics of magnetic reconnection, focusing on significant results in the past decade from dedicated laboratory experiments, numerical simulations, and space astrophysical observations. Particularly in the area of local reconnection physics, many important findings have been made with respect to two-fluid dynamics, the profile of the neutral sheet, the effects of guide field, and scaling laws with respect to collisionality. Notable findings have been made on global reconnection dynamics through detailed documentation of magnetic self-organization phenomena in fusion plasmas as well as in solar flares. After a brief review of the well-known early work, we will discuss representative recent experimental and theoretical work and attempt to interpret the essence of significant modern findings. Especially, the recent data on local reconnection physics from the Magnetic Reconnection Experiment device [M. Yamada *et al.*, *Phys. Plasmas* **13**, 052119 (2006)] are used to compare experimental and numerical results. © 2007 American Institute of Physics. [DOI: [10.1063/1.2740595](https://doi.org/10.1063/1.2740595)]

I. INTRODUCTION

Magnetic reconnection, a topological rearrangement of magnetic field lines, is key for self-organization processes in plasmas.^{1–16} During magnetic reconnection, a conversion of magnetic energy to plasma kinetic energy occurs by way of acceleration or heating of plasma particles. Magnetic reconnection is seen in the evolution of solar flares, in the dynamics of the Earth's magnetosphere, and is considered to occur in the formation process of stars. It also occurs as the self-organization process in current-carrying fusion plasmas, and it plays a key role in major and minor disruptions of tokamak discharges and in the relaxation processes in reversed field pinch (RFP) plasmas.⁴

Solar flares are perhaps the best-known example of magnetic reconnection. Since the concept of magnetic reconnection originated from solar flares, it has been considered to play a major role in the evolution of solar coronas as well as in coronal mass ejections (CME).^{7–11} CMEs are considered to be produced by loss of equilibrium in a coronal magnetic plasma configuration, which induces abrupt changes in magnetic topology. Magnetic reconnection has been attributed to the observed eruptive phenomena and to their associated flares, ultraviolet emissions, and soft and hard X rays. The recent observations from the YOHKOH,^{7,8} SOHO,⁹ TRACE,¹⁰ and RHESSI¹¹ satellite missions have confirmed that magnetic reconnection is indeed the fundamental process operating in powerful solar eruptions—flares and coronal mass ejection—that typically result in the efficient acceleration of particles to high energies.

Magnetic reconnection plays an important role during interactions between the magnetic fields of the solar wind

and the Earth's dipole field in both the day-side (magnetopause) and the night-side of the magnetosphere (magnetotail).^{12–14} Since the observed thickness of the neutral sheath is on the order of the ion skin depth or the ion gyroradius, the reconnection dynamics cannot be described by the conventional magnetohydrodynamic (MHD) theory of reconnection. This is because ions and electrons behave differently in the reconnection region requiring two-fluid physics, and the reconnection can be a very turbulent process both in time (intermittent) and space (patchy). A number of researchers have observed electric and magnetic turbulence in the magnetopause as well as in the magnetotail.

Reconnection is also considered to play a key role in star formation and the generation of anomalously fast accretion of galaxies.⁵ In this context, reconnection is thought to be the mechanism for releasing energy in stellar flares and accretion disks, and may provide a level of heating and particle acceleration observed in the coronas of these systems. Because of a large induced electric field created by reconnection, the presence of high-energy particles, 1 GeV in solar coronas and 10^{17} eV in the Crab pulsar, could be explained by magnetic reconnection.¹⁵ Protostar disks, which are thought to be made of partially ionized gas, can increase their accretion rate through fast magnetic reconnection processes.

In recent decades, several dedicated laboratory experiments for magnetic reconnection research were built and operated to provide important data contributing to the understanding of the fundamental physics of reconnection.¹⁶ These experiments can create fundamental physics processes in a controlled manner and provide well-correlated plasma parameters at many plasma locations simultaneously, compensating for the major drawbacks of satellite measurements, which are limited to one or a few simultaneous locations. The present paper presents examples of how these laboratory

^{a)}Paper CT1 1, *Bull. Am. Phys. Soc.* **51**, 58 (2006).

^{b)}Invited speaker.

plasma studies have contributed importantly to the fundamental understanding of the interaction of space and astrophysical plasmas with magnetic fields.

The fundamental mechanisms of magnetic reconnection are analyzed through (i) local and (ii) global perspectives. In local analysis, it is viewed that reconnection mechanisms are determined primarily by local plasma parameters in the reconnecting region; the Sweet-Parker^{17,18} and Petschek models¹⁹ use such an assumption. However, reconnection is generally influenced and determined by external boundary conditions or the initial three-dimensional (3D) global configuration and topology. For example, a global MHD instability caused by external conditions can drive a magnetic reconnection changing plasma topology and determining the reconnection rate. In tokamak plasmas, it is found that a large MHD instability caused by external conditions can drive 3D magnetic reconnection and can determine the reconnection rate. The actual reconnection phenomena are generally determined both by local plasma properties, which are often governed by physics beyond MHD, and by global plasma characteristics, which are generally described satisfactorily by MHD. In this paper, we describe major progress in both aspects.

Theory on reconnection,^{1-5,17-19} which started with observations in solar coronas and in the Earth's magnetosphere, dominated early research in this subject, while present research is dominated by experiments, satellite observations, and numerical simulation, with theory playing a supporting role. Since the early work is well presented in textbooks and space is limited for this paper, more emphasis will be placed on recent experimental and simulation work, focusing on recent major findings that have an important impact on broad cross-discipline reconnection research.

One of the most important questions has been why reconnection occurs much faster than predicted by classical MHD theory. In the past 15 years, significant advances in understanding the local physics of magnetic reconnection have been made through numerical simulations, observations from satellites, and dedicated laboratory plasma experiments. Recent theoretical²⁰⁻²⁴ and experimental work^{16,25-29} has revealed that two-fluid effects, due to the different behavior of ions and electrons, are important within the critical layer where reconnection occurs. Two-fluid effects are now considered to affect the rate at which reconnection occurs in the magnetosphere, fusion plasmas, and even in stellar flares. Recent data from dedicated laboratory experiments show striking similarity to current magnetospheric measurements, in which both two-fluid Hall effects and magnetic fluctuations are detected together. This paper compares the results from these two fields.

While reconnection often involves change in global topology, analysis of global characteristics of magnetic reconnection has been less developed. This is partly because it is difficult to monitor the plasma parameters of an entire region including boundaries. Since the launch of the recent successful solar satellites, abundant new information has improved our understanding of magnetic reconnection in solar flares. In the magnetopause, intermittent flux transfer events were recorded by space satellites and interpreted in terms of global

relaxation phenomena. In fusion research, magnetic reconnection is studied intensively through magnetic relaxation phenomena in toroidal pinch devices. In this paper, the global properties of magnetic reconnection are discussed by citing examples from the recent results on magnetic self-organization in laboratory plasmas, such as relaxation phenomena in tokamak and RFPs.

There still exist many different views concerning which physical processes are most important for reconnection. It has only been recently realized under what condition two-fluid effects become dominant over the classical MHD rate.²⁸ Yet it is not clear how boundary conditions affect the local reconnection rate. Whether two-fluid Hall processes or anomalous resistive processes are most important is still being debated. Examples of analysis based on these different views will also be presented. Finally, it should be noted that this is not a comprehensive review of ongoing research on magnetic reconnection, and the author apologizes for omitting some important ongoing works because of limitation of space and of the author's knowledge. Section II briefly reviews the historical development of reconnection research. Sections III and IV describe the recent major findings on local and global reconnection physics, respectively. Section V presents a summary and important future research issues.

II. HISTORICAL DEVELOPMENT OF THEORY AND OBSERVATIONS

How do magnetic field lines move around in plasmas and how do they reorganize? The ideal MHD, which was developed in the early 1950s, describes the dynamics of highly conductive plasmas ($\eta=0$), where $E_{\parallel}=\mathbf{E}\cdot\mathbf{B}/B=0$,¹⁻⁵ and magnetic field lines always move with plasma and remain intact. If we consider magnetic field lines that are approaching each other in a plasma, magnetic field gradients become locally strong at the encountering point. Plasma flows can lead to singular current density sheets where E_{\parallel} becomes sufficiently large inducing non-MHD plasma behavior so that a magnetic field line can lose its original identity. Dungey showed³⁰ that such a current sheet can indeed be formed by the collapse of magnetic field near an X-type neutral point, and he suggested that "lines of force can be broken and rejoined." When the field lines are reconnected, the topology of the magnetic configuration can change and large $\mathbf{j}\times\mathbf{B}$ MHD forces often result. Can we describe how the magnetic energy is converted to plasma heating or acceleration in complex 3D systems?

Sweet and Parker addressed magnetic reconnection problems in a situation in which solar coronas are merging and transformed the reconnection region into a two-dimensional reconnection boundary layer in which oppositely directed field lines merge as shown in Fig. 1. In their model, magnetic fields of opposite polarity approach in the reconnection region where they merge, and newly reconnected field lines emerge and move away. This 2D model introduced an important concept that magnetic reconnection rate can be calculated quantitatively through a magnetic flux transfer (which can be straightforwardly defined in 2D) be-

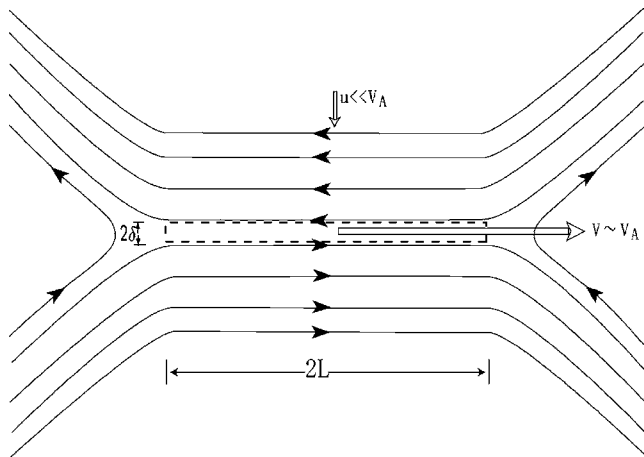


FIG. 1. Sweet-Parker reconnection model.

tween two geometrically separated plasma regions, assuming uniformity in the third dimension.

While the question remains whether global multiple reconnections can be analyzed by such a singular localized boundary layer, let us proceed with analysis of the local reconnection layer using resistive MHD formulation. In the one-fluid MHD formulation, the motion of magnetic field lines in a plasma can be described by combining Ohm's law,

$$\mathbf{E} + \mathbf{v} \times \mathbf{B} = \eta \mathbf{j}, \quad (1)$$

and Maxwell's equations to yield

$$\partial \mathbf{B} / \partial t = \nabla \times (\mathbf{v} \times \mathbf{B}) + (\eta / \mu_0) \nabla^2 \mathbf{B}. \quad (2)$$

Here, conventional notations are used for the local electric and magnetic field vectors, \mathbf{E} , \mathbf{B} , current density, \mathbf{j} , and plasma flow velocity, \mathbf{v} . When $\eta=0$, magnetic field lines move with the fluid without any dissipation as described by Eq. (2). In resistive MHD plasmas, hydromagnetic flows can lead to the formation of a neutral sheet where the plasma flow is reduced to a finite size and the electric field (\mathbf{E}) is balanced with $\eta \mathbf{j}$ in Eq. (1). In the diffusion region shown in Fig. 1, the resistivity becomes sufficiently large that a magnetic field line can diffuse, lose its original identity, and *reconnect* to another field line. Utilizing the continuity equation and pressure balance between the upstream ($p \sim B^2/2\mu_0$) and the downstream ($p \sim \rho v^2/2$) regions, Parker and Sweet derived a very simple formula for reconnection speed V_R :

$$V_R/V_A = \delta/L = 1/\sqrt{S}, \quad (3)$$

where $S = \mu V_A L / \eta$ is the Lundquist number, the ratio of the Ohmic diffusion time to the crossing time of the Alfvén waves.

In the resistive MHD formulation of Sweet and Parker, magnetic fields diffuse and dissipate in the rectangular reconnection region, where incoming plasma flux is balanced with the outgoing flux, satisfying a continuity equation for plasma fluid. The reconnection rate depends on S , with S being usually extremely large: S can be 10^3 – 10^8 in laboratory fusion plasmas, 10^{10} – 10^{14} in solar flares, and 10^{15} – 10^{20} in the Galaxy. This Sweet-Parker reconnection rate is far too slow to

explain reconnection phenomena in flares, star formation, or dynamos. For example, in actual solar flares energy release (which is considered due to reconnection) occurs much faster (<1 h) than the Sweet-Parker time (0.1–1 year). By the Sweet-Parker model, star formation, which is considered to involve magnetic reconnection, would take much longer than the entire lifetime of the Universe.⁵ This slowness comes from the assumption of this model that plasma and magnetic flux have to pass through the narrow neutral sheet with a thickness of $\delta = L/S^{-1/2}$ as shown in Fig. 1.

At about the same time, another important MHD theory was developed by Furth *et al.*³¹ to quantitatively calculate the growth of the resistive tearing mode in a 2D current sheet for the analysis of tearing instability in tokamak plasmas. But this theory, based also on resistive MHD, does not resolve the problem that the reconnection occurs in too slow a time scale.

To explain the observed fast reconnection, an anomalous resistivity theory has often been used employing an *ad hoc* enhanced value of the resistivity in Eqs. (1) and (2) to yield

$$\mathbf{E} + \mathbf{v} \times \mathbf{B} = \eta_s \mathbf{j} + \eta_{\text{anom}} \mathbf{j} = \eta_{\text{eff}} \mathbf{j}, \quad (1')$$

$$\partial \mathbf{B} / \partial t = \nabla \times (\mathbf{v} \times \mathbf{B}) + (\eta_{\text{eff}} / \mu_0) \nabla^2 \mathbf{B}. \quad (2')$$

Although it is difficult to build a sound theoretical basis for uniformly enhanced resistivity based on turbulence or other mechanisms, this formulation is effective in describing the fast reconnection rate by MHD. Recently, a generalized Sweet-Parker model was developed to quantitatively explain the reconnection rates observed in a laboratory plasma in the Magnetic Reconnection Experiment (MRX).^{32,33}

Shortly after the Sweet-Parker theory was developed, another model was proposed by Petschek¹⁹ to resolve the dilemma of the slow reconnection rate, introducing shocks that open up the neutral sheet into a wedge shape. By eliminating the flow limiting outgoing current channel as shown in Fig. 2(a), this model leads to a much faster rate of reconnection. While the Petschek reconnection rate has been consistent with the observed fast reconnection rates in space and has become very frequently cited, it has not yet been rigorously established because it is not compatible with resistive MHD characteristics.³

In the past two decades, a new development of this model has been made by employing a locally enhanced resistivity, $\eta_{\text{eff}}(\mathbf{r})$, which is consistent with the notion that the electron current should encounter an anomalous resistivity due to the waves generated by high electron current density in the reconnection region.^{34–37} In this case, Eq. (2) has to be modified¹ as

$$\begin{aligned} \partial \mathbf{B} / \partial t = & \nabla \times (\mathbf{v} \times \mathbf{B}) + (\eta_{\text{eff}} / \mu_0) \nabla^2 \mathbf{B} \\ & + (1/\mu_0) \nabla \eta_{\text{eff}} \times (\nabla \times \mathbf{B}). \end{aligned} \quad (2'')$$

The locally enhanced resistivity expressed in the second and third terms of the right side increases dissipation near the X point, generating a wedge-shaped reconnection region with “slow shocks” formed near the central high resistivity region as shown in Eq. (2'').³⁶ This configuration is free from the constraint of the thin reconnection layer of the Sweet-Parker

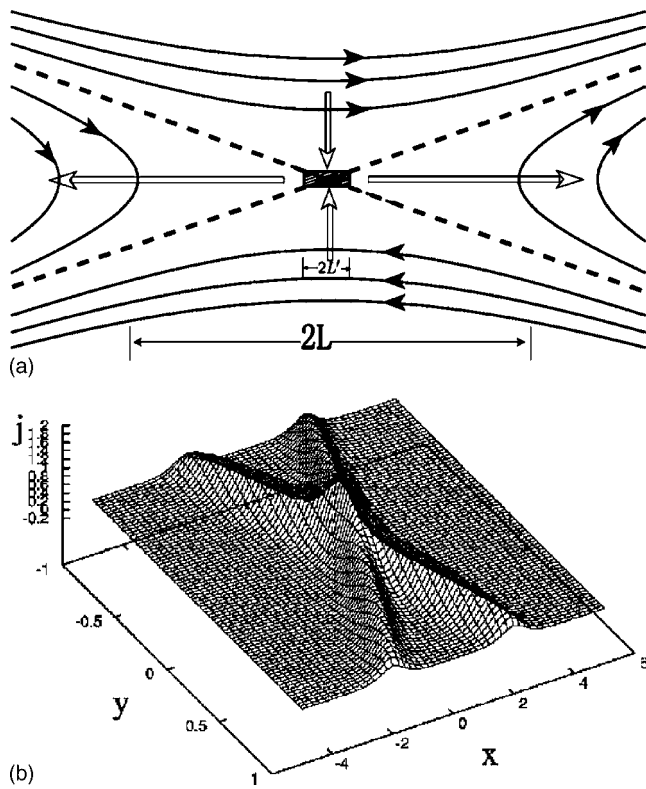


FIG. 2. (a) Petschek reconnection model (Ref. 19). (b) Current profile from a numerical simulation using a locally enhanced resistivity (Ref. 36).

model and allows for a fast reconnection rate. However, to date there has been no conclusive experimental evidence of shocks observed in association with the magnetic reconnection layer in laboratory plasmas.

In the early phase of reconnection research, magnetic reconnection was described primarily through the MHD theories such as those mentioned above, which treat the plasma as a single fluid.^{17–19} The MHD framework is based on the assumption that electrons and ions move together as single fluid even in the presence of internal currents. This formulation has been reevaluated by the realization that the MHD condition does not hold in a thin reconnection layer such as those created in the magnetosphere, in which ions become demagnetized and the relative drift velocity between electrons and ions can be very large. Reconnection layers such as those created at the magnetopause^{12–14} have thicknesses that are comparable to the ion skin depth (c/ω_{pi}). In this $\beta \sim 1$ region, the ion skin depth is comparable to the ion gyroradius and only electrons are magnetized, leading to a strong Hall effect. This effect is considered responsible for speeding up the rate of reconnection. Since the two-fluid effects are due to the different behaviors of large orbit ions and strongly magnetized electrons with small orbits, electromagnetic or electrostatic turbulence at high frequency ($\omega > \omega_{ci}$) can be excited and can increase the magnetic reconnection rate.

In the two-fluid formulation, Ohm's law of Eq. (1) should be replaced by the generalized Ohm's law, which describes the force balance of an electron flow, namely,

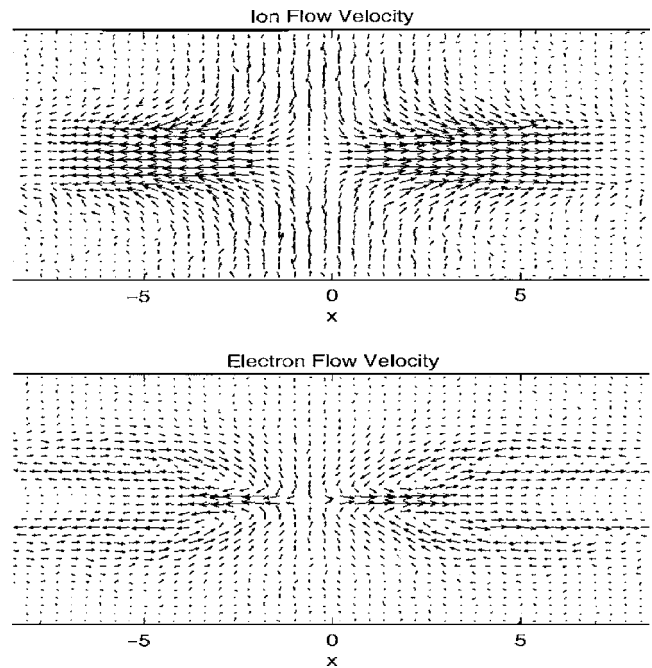


FIG. 3. Patterns of ion and electron flows in the neutral sheet (Ref. 24).

$$\mathbf{E} + \mathbf{v} \times \mathbf{B} = \eta_s \mathbf{j} + (\mathbf{j} \times \mathbf{B})/ne + m_e j_e (\partial \mathbf{v}_e / \partial t + \mathbf{v}_e \cdot \nabla \mathbf{v}_e) - \nabla \cdot \mathbf{p}_e / en, \quad (4a)$$

or

$$\mathbf{E} + \mathbf{v}_e \times \mathbf{B} = \eta_s \mathbf{j} + m_e j_e (\partial \mathbf{v}_e / \partial t + \mathbf{v}_e \cdot \nabla \mathbf{v}_e) - \nabla \cdot \mathbf{p}_e / en. \quad (4b)$$

Here, the conventional notations are again used with electron flow velocity, \mathbf{v}_e , and perturbative electron pressure tensor, \mathbf{p}_e ; $\mathbf{p}_e = \langle (\mathbf{v}_e - \langle \mathbf{v}_e \rangle)(\mathbf{v}_e - \langle \mathbf{v}_e \rangle) \rangle$. Generally in Eq. (4a), all vectors should generally include fluctuation components; η_s denotes the classical Spitzer resistivity based on Coulomb collisions. In a thin reconnection layer in which the ions and electrons do not move together, new effects associated with the Hall term in the generalized Ohm's equation [the second term on the right-hand side (RHS) of Eq. (4a) or the second term of the LHS of Eq. (4b)] contribute to increased electric field in the direction of sheet current. This large electric field ($E = -d\Psi/dt$) is translated to the fast motion of flux lines in the reconnection plane, or a fast rate of magnetic reconnection.

In the past ten years, two- or three-dimensional numerical simulations^{20–24} of the collision free neutral sheet based on two-fluid or kinetic codes demonstrate the importance of the Hall term $\mathbf{j} \times \mathbf{B}$ through a steady (laminar) cross-field current of electrons, which contribute to a large apparent resistivity and generate fast reconnection. The extensive numerical work by Drake *et al.*^{20,23} and Horiuchi and Sato²¹ was followed by many with periodic and open boundary conditions. Figure 3 shows the most recent result from particle-in-cell (PIC) simulation by Pritchett²⁴ on the dynamics of ions and electron flows in a typical neutral sheet. As seen in the figure, the ions, which become unmagnetized as they enter the neutral sheet, are accelerated across the sheet, and

then turn and flow outward nearly parallel to the exit direction. In contrast, the magnetized electrons mainly flow inward along the separatrices toward the X point. As the electrons' $\mathbf{E} \times \mathbf{B}$ motion makes them migrate toward the X line, the magnetic field weakens. The electrons' drift (E_y/B_x) becomes larger near the X point and the electrons are ejected out to the exit. This electron flow pattern shown in Fig. 3 generates net circular currents in the reconnection plane and thus creates an out-of-plane magnetic field with a quadrupole profile;³⁷ this effect has been regarded as a signature of the Hall effect. The increased electric field caused by the strong Hall term $\mathbf{j} \times \mathbf{B}$ through a steady laminar cross-field current of electrons is interpreted as a fast motion of flux lines ($E = -d\Psi/dt$) in the reconnection plane, or a fast rate of magnetic reconnection. It should be noted, however, that the Hall term alone does not create dissipation, which is essential for conversion of magnetic energy to particle kinetic energy.

Measurement of the exact profiles of the neutral sheet provides a clue to the understanding of the two-fluid physics mechanisms working on the reconnection region. Confirmation of the Hall effects has been recently reported as detection of the Hall magnetic field²⁶⁻²⁹ in both space and laboratory plasmas. The Polar satellite crossed the magnetopause in a southward interplanetary magnetic field (IMF) situation and presented a typical example of the fine structure of the neutral sheet²⁶ with an out-of-reconnection plane magnetic field, a signature of Hall effects. More conclusive and precise measurements of Hall effects in the neutral sheets were carried out in MRX and SSX in the past few years.²⁷⁻²⁹ In addition, electrostatic and electromagnetic fluctuations were observed in MRX around the lower hybrid frequencies at the edge and the center of the current sheet, respectively, with the electromagnetic waves correlating well with the enhanced resistivity. It is very important to find the relationship between the Hall effects caused by laminar electron flows and these high-frequency fluctuations.

We note here that in recent literature, two mechanisms have often been cited as possible causes for fast reconnection: anomalous resistivity generated by plasma turbulence and the Hall effect of two-fluid theory. We note that these two phenomena can both be considered as two-fluid effects in a broad sense. Equation (4a) can be expressed in a similar form to that of the resistive MHD, if we express the right-hand side as $\eta_s \mathbf{j} + \eta_{\text{anom}} \mathbf{j} = \eta_{\text{eff}} \mathbf{j}$. The crucial fluctuation components in $\mathbf{j}_e \times \mathbf{B} + m_e l e (\partial \mathbf{v}_e / \partial t + \mathbf{v}_e \cdot \nabla \mathbf{v}_e) - \nabla \mathbf{p}_e / \epsilon n - e n \mathbf{E} / \epsilon n_0$, are (nonlinearly) proportional to the driving term, the electron current density \mathbf{j}_e ($\sim \mathbf{v}_e$), and can be expressed together as $\eta_{\text{anom}} \mathbf{j}_e$. We note that the fluctuation-induced resistivity should include $\langle n_1 E_{1y} \rangle / n_0$, where n_1 and E_1 are fluctuating density and electric field, and n_0 is the averaged density. Thus, in the MHD formulation with an effective resistivity, the Hall effect in the neutral sheet and various fluctuations contribute together to generate $\eta_{\text{anom}} \mathbf{j}_e$. An important task is to create a controlled environment in which one dominant effect is isolated from the rest and can be investigated separately.

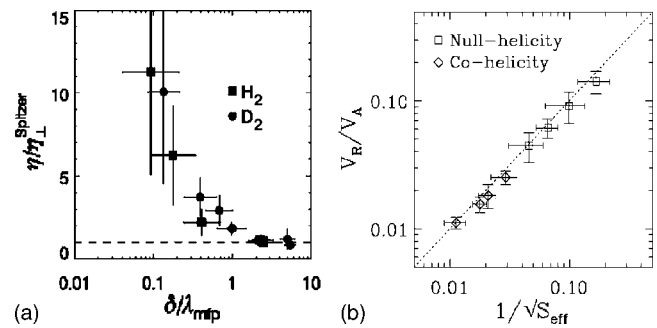


FIG. 4. (a) Effective resistivity normalized by the perpendicular Spitzer value vs collisionality, $\delta/\lambda_{\text{mfp}}$ (Ref. 38). (b) MRX data for reconnection speed and generalized Sweet-Parker scaling (Ref. 33). Cohelicity reconnection occurs with sizable guide field ($B_G \sim 2B_{\text{reconn}}$) (Ref. 47).

III. RECENT DISCOVERIES AND FINDINGS ON LOCAL RECONNECTION PHYSICS

A. Reconnection rate versus collisionality: Reduced collisions enhance the reconnection rate

For decades, one of the most important questions has been why reconnection occurs much faster than predicted by classical MHD theory. In many dedicated experiments for magnetic reconnection study, local reconnection physics have been studied extensively. Reconnection rates have been measured in both collision-dominated and collision-free plasmas.^{32,33} In the collisional regime, the reconnection rate was found to be in good agreement with the classical Sweet-Parker theory based on the transverse Spitzer resistivity.^{33,38} In Spitzer's calculation, the transverse resistivity for electrons is twice the parallel resistivity. The measured resistivity values verified this theoretical number within 30% error and they vary as $(T_e)^{-3/2}$, as expected. In the relatively collision-free regime where the mean free path is much longer than current sheet thickness, significant resistivity enhancement (by more than a factor of 10) over the classical values was measured as shown in Fig. 4(a). The measured reconnection electric field, which represents ($E = -d\Psi/dt$), increases as the collisionality is reduced. This is not consistent with the collision-based reconnection model.

Despite the long history and influence of Sweet-Parker theory, the model had never been exactly tested either in a laboratory plasma or in space until the first quantitative study was carried out in MRX in 1998.^{32,33} All basic plasma parameters were measured including the magnetic field profile, electron density, electron temperature, and reconnection speed V_R . Although the detailed structures of reconnection layers differ depending on the presence of a guide-field or collisionality, a common feature was that the formed current sheet was generally stable and axisymmetric. The classical Sweet-Parker model did not agree at all with the observed reconnection rates measured in the wide range of collisionality in MRX. However, a generalized Sweet-Parker model, which incorporates compressibility, downstream pressure, and the effective resistivity, η^* , can well explain the observed reconnection rate. In this generalized model, the reconnection rate is given as

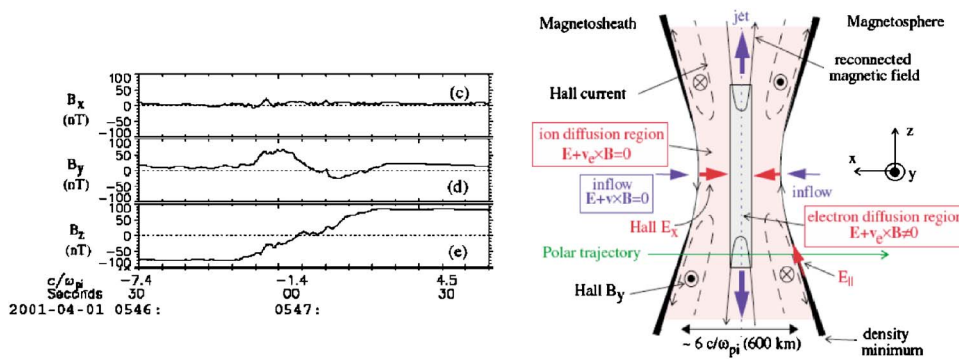


FIG. 5. (Color online) (Left) Detected magnetic field components vs time (distance). (Right) Conjectured flight pass of the Polar satellite in the modeled diffusion region (Ref. 26).

$$V_R/V_A = 1/\sqrt{S_{\text{eff}}}, \tag{5}$$

where

$$S_{\text{eff}} = \frac{\mu_0 L V_A}{\eta^*} \frac{1}{1 + L \dot{n}/n V_z} \frac{V_A}{V_z} \tag{5a}$$

Figure 4(b) shows good agreement between the observed reconnection rate and the prediction by the generalized model, $V_R/V_A = 1/\sqrt{S_{\text{eff}}}$. A significant implication of this result is that the Sweet-Parker model with generalizations can be formulated for a stable 2D reconnection neutral sheet with axisymmetric geometry.

This generalized Sweet-Parker model applies to both cases with and without a guide-field (cohelicity and null-helicity, respectively). The observed slower reconnection rates with a guide field are found to be attributed to (i) smaller resistivity enhancement, (ii) higher downstream pressure, and (iii) less compressibility due to a guide field. The first factor (i) could be because the current flows along field lines with fewer high-frequency fluctuations and fewer Hall effects. The second and third factors can be understood as effects due to the existence of a toroidal field, which can help confine the plasma locally to increase downstream pressure and reduce plasma compressibility.

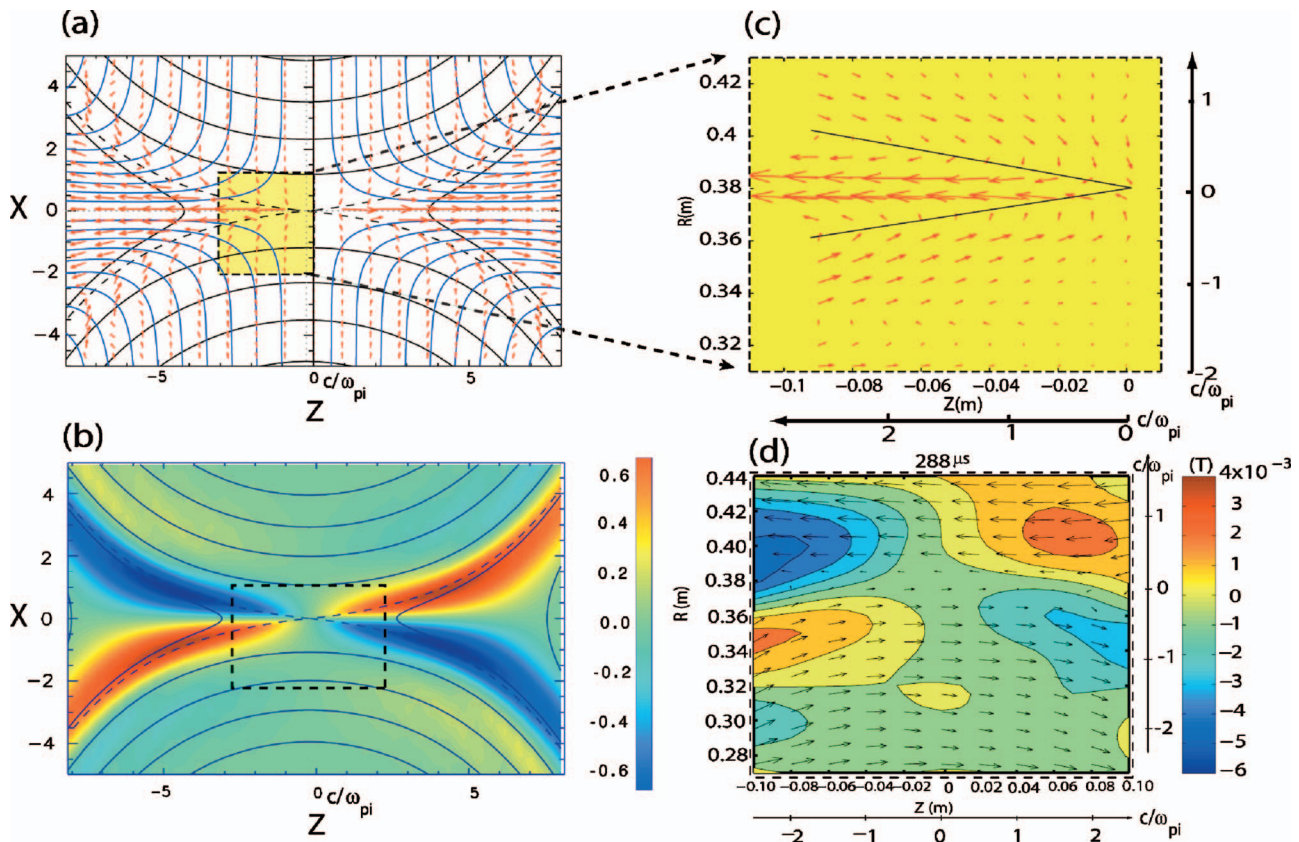


FIG. 6. (Color) Comparison simulation and experiments: (a) Calculated patterns of ion (blue lines) and electron (red arrows) fluid flows superposed on the flux plot of reconnection field lines (black). The coordinates are in units of $d_1 = c/\omega_{pi} = 1.0$. (b) Out-of-plane quadrupole (B_1) is shown in color contours with in-plane magnetic field lines. (c) Comparison of 2-D profiles of Hall current measured in MRX with the yellow-coded region in the figure (a) for the same spatial coverage in terms of c/ω_{pi} . (d) The magnetic field in the diffusion region for D plasmas: $c/\omega_{pi} = 4$ cm. The arrows depict the measured magnetic field vectors in the reconnection (x, z) plane. The size of the arrows normalized to the maximum strength, 300 gauss. The color-coded contour plot shows the out-of-plane magnetic field.

B. Verification of Hall effects in the neutral sheet

The two-fluid dynamics of reconnection, which are illustrated in Fig. 3,²⁴ predicts the presence of strong Hall effects due to the decoupling of electrons' flow from that of ions. In a collision-free neutral sheet such as that seen in the magnetosphere, magnetized electrons tend to pull magnetic field lines in the direction of the electron current generating an out-of-plane quadrupole field.

In the magnetosphere, the two-fluid physics of magnetic field reconnection was recently analyzed in terms of the ion diffusion region of scale size $c/\omega_{pi} \sim 100$ km at the subsolar magnetopause. Strong evidence of the ion diffusion region in the collisionless two-fluid regime was reported at the subsolar magnetopause and compared by Mozer *et al.*²⁶ with Hall MHD theory. When the Polar satellite crossed through the magnetopause region, a typical hyperbolic tangent configuration of a reconnecting in-plane field and a sinusoidal out-of-plane Hall magnetic field was clearly identified near the separatrices of the current sheet, as shown Fig. 5.

A detailed quantitative study of Hall effects has been carried out by the MRX group by comparing the results of a two-fluid simulation for MRX geometry and the experimental results.^{27,28} Aided by the numerical work,³⁹ a basic understanding of the two-fluid reconnection dynamics has been made as follows.

As is shown in the simulation, Fig. 6(a), the reconnecting field lines move into the neutral sheet (reconnection layer) of width comparable to the ion skin depth, and as they approach the X point (the center of the reconnection plane), ions become demagnetized. The ion flows gradually change their direction by 90 degrees, from the x to the z direction in the reconnection (x, z) plane (as shown by the blue line). It is shown that magnetized electrons flow quite differently (as shown in red color vectors) still following magnetic field lines until they approach the X point (strictly speaking, the "X line" in 3D geometry) or separatrix lines (likewise separatrix surfaces in 3D geometry). As the electron's $E_y \times B_z$ motion (E_y is the out-of-plane electric field that drives reconnection) makes them migrate toward the X line, the magnetic field weakens and the electron's drift (E_y/B_z) becomes larger near the X line and the electrons are ejected out to the exit. The electron flow pattern shown in Fig. 6(a) generates a circular net current pattern in the reconnection plane and thus creates an out-of-plane magnetic field with a quadrupole profile as shown in Fig. 6(b). This effect has been regarded as a hallmark of the Hall effect.²⁰⁻²⁴ Recently Uzdensky and Kulsrud calculated this out-of-plane field analytically.³⁷ This process can be interpreted as a mechanism in which the electrons, which are flowing in the y direction of the neutral sheet current, tend to pull magnetic field lines toward the direction of electron sheet current, the y direction.

Figures 6(c) and 6(d) present experimentally measured profiles of in-plane electron flow vectors and out-of-plane magnetic field recorded by a fine-structure probe array inserted in the plasma.^{27,28} An out-of-plane field with a quadrupole profile, a signature of Hall effects, was observed in MRX as shown in Fig. 6(d),²⁷ in agreement with the numerical simulation. The circular electron flow patterns around the

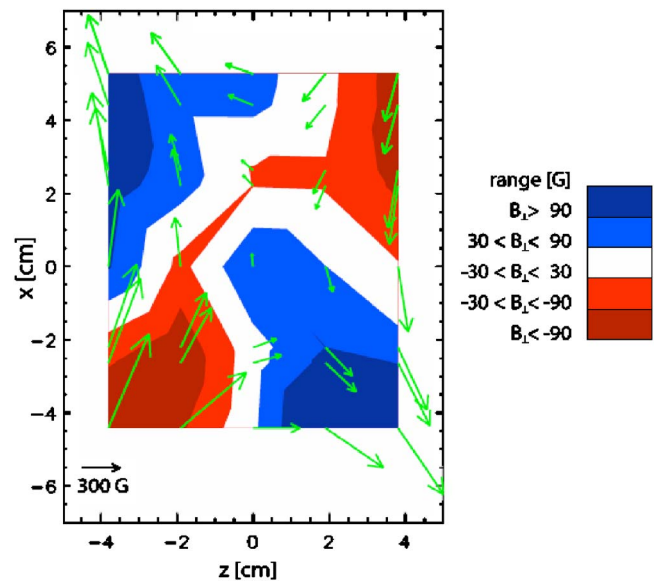


FIG. 7. (Color online) Measured quadrupole field in SSX. Reconnection is driven by two toroidal plasmas moving parallel to the z axis (Ref. 29).

separatrix lines in the reconnecting plane were deduced by measuring the fine structure of out-of-plane components of the reconnecting magnetic field. To deduce the electron flow vectors from $\text{Curl } B_y = j(x, z)$, ions are assumed to move much slower than electrons, which was verified in the earlier measurements.³³ The data from MRX provide the most conclusive demonstration of Hall effects through a detailed quantitative comparison of the experimental data with numerical simulation results.

In a somewhat different geometry of the plasma merging experiment SSX (Swarthmore Spheromak Experiment),²⁹ the observation of a similar out-of-plane field was reported as shown in Fig. 7. While it was argued that an in-plane Hall electric field was measured based on the $\mathbf{j} \times \mathbf{B}$ force balance, their data was not consistent with others.⁵¹ A direct measurement of plasma space potential and the important in-plane pressure gradient would verify their argument. The similarities of these laboratory experimental results and space data have resulted in closer collaborations between the laboratory and space physicists.

In the MST (Madison Symmetric Torus) reversed field pinch⁴⁰ device, an experimental measurement of the collisionless reconnection region with a strong guide field was also carried out in the center core using laser Faraday rotation and in the edge with magnetic probes. In the plasma core, the magnetic field measured by Faraday rotation of a far-infrared laser indicated that the Hall effect is strongly localized to the reconnection layer of a helical structure.

A major difference between the Hall MHD fields observed in the ion diffusion region in laboratory and space measurements is that such clear signatures occur in the Earth's magnetosphere less than 1% of the time. This may be because the space geometry is not as globally symmetric as that in the laboratory plasma, the space structures are three dimensionally unstable, the space measurements are generally made far from the X line, or because of time depen-

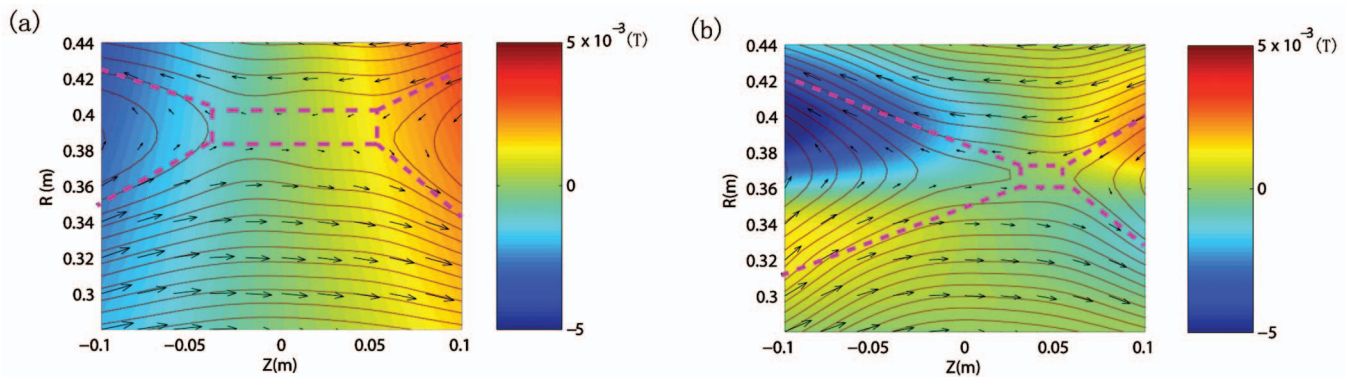


FIG. 8. (Color) Comparison of the neutral sheet configuration as described by measured magnetic field vectors and flux counters for high- (collisional) and low-density cases: (a) Collisional regime ($\lambda_{\text{mfp}} \sim 1 \text{ mm} \ll \delta$); (b) near collision-free regime ($\lambda_{\text{mfp}} \sim 1 \text{ cm} \sim \delta$). Out-of-plane fields are depicted by the color codes range $-50 < B_y < 50 \text{ G}$.

ences in the space measurements. There has been some evidence of electron diffusion regions at the subsolar magnetopause.⁴¹ Apparently measured electron diffusion regions appear throughout the magnetopause and at the separatrices, but intermittently. Comparisons of these high spatial and temporal resolution laboratory measurements with existing and future analyses of space data will provide important information for planning the orbit and data collection strategies for space missions.

C. Measurements of the shape of the reconnection layer: The 2D profile of the reconnection layer drastically changes with respect to collisionality together with the reconnection rate

The profile of a neutral current sheet manifests the key physics of magnetic reconnection. The essential physics of reconnection can be studied by generating a prototypical reconnection layer in dedicated laboratory experiment. In a driven reconnection in MRX, profiles of the neutral sheets have been investigated by changing collisionality, which depends on the plasma density and temperature. It is observed that the 2D profile of the neutral sheet is changed significantly from the rectangular shape in the collisional regime ($\lambda_{\text{mfp}} \ll \delta_{\text{sheath}}$) to a double wedge shape in the collision-free regime ($\lambda_{\text{mfp}} > \delta_{\text{sheath}}$) as the collisionality is reduced and the reconnection rate increases.²⁸ Figure 8 shows how the profile of the MRX neutral sheet changes with respect to the colli-

sionality condition by comparing the neutral sheet configurations described by the measured magnetic field vectors and flux contours. In the high plasma density case, as shown in Fig. 9(a), where the mean free path is much shorter than the sheet thickness, a rectangular-shaped neutral sheet profile of the Sweet-Parker model of Fig. 1 type is identified, and the classical reconnection rate is measured. In the case of low plasma density, where the electron mean free path is longer than the sheet thickness, a double-wedge-shaped sheet profile appears, as shown in Fig. 8(b), and the Hall MHD effects become dominant, as indicated by the notable out-of-plane quadrupole field depicted by the color code. There is no recognizable out-of-plane Hall field in the collisional case of Fig. 8(a). The weak dipole toroidal fields profile seen in Fig. 8(a) is considered to be a remnant of the field created by initial poloidal discharges around the two flux cores. A double-wedge profile of the Petschek type, seen in Fig. 9(b), deviates significantly from that of the Sweet-Parker model [Fig. 8(a)], and a fast reconnection rate is measured in this low collisionality regime. The MRX result is an important experimental demonstration to show how collisionality changes the shape of the reconnection layer simultaneously affecting the reconnection rate. However, to date, a slow shock, a key signature of the Petschek model, has not been identified even in this regime.

In the past decade, many numerical simulations were carried out using the resistive MHD and two-fluid MHD

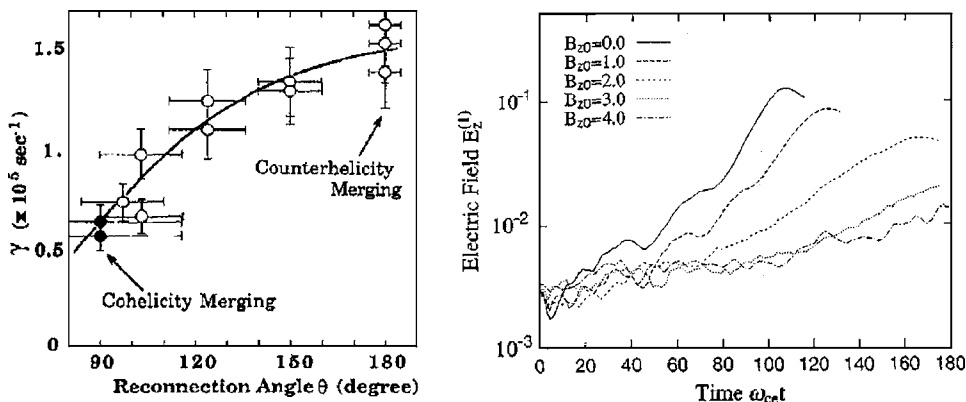


FIG. 9. Guide field effects: (a) Reconnection rate $[(d\Psi/dt)/\Psi]$ vs merging angle of field lines measured in TS-3 (Ref. 46); (b) reconnection rate expressed by the electric field $(d\Psi/dt)$ vs time for different guide-field strengths (normalized by the reconnecting field) (Ref. 54).

codes.^{3,20–24,42,43} When resistivity was uniform in space and sufficiently large, the familiar rectangular-shaped Sweet-Parker layer was obtained. When the resistivity becomes small as collisionality is reduced, characteristic features of the two-fluid dynamics appear with the double-wedge shaped neutral sheet. Ma and Bhattacharjee reported a result from their numerical simulation that the neutral sheet profile changed from a double Y shape to an X shape with impulsive reconnection features as two-fluid effects were turned on with a constant resistivity.⁴² Cassak *et al.* has recently found a nonreversible transition by varying resistivity.⁴⁴ Without a guide field, the measured profile of the MRX neutral sheet is in remarkable agreement with the results of numerical simulations.^{42,22–24}

It is very difficult to directly measure the exact spatial profiles of the reconnection region or neutral sheet in the magnetosphere, because of the limited number of measuring locations by satellites. In solar atmosphere, 2D neutral sheet-like patterns have been recognized sometimes through soft-x-ray satellite images, but their exact magnetic profiles are unknown. It appears that a reconnection process is underway throughout this area. In order to describe the observed reconnection rate by the Sweet-Parker model, the plasma resistivity or energy dissipation has to be anomalously large throughout a wide region in order to explain the apparent fast flux transfer. While MHD turbulence is attributed to this observed fast reconnection, there is no conclusive evidence.

D. Effects of a guide field: A guide field reduces the reconnection rate in 2D reconnection geometry

At the magnetopause, magnetic reconnection plays a central role in the interaction between the solar wind and the Earth's dipole field. Dayside reconnection in the terrestrial magnetosphere^{13,14} is depicted as a series of “flux transfer events” and has a strong dependence on the merging angle of field lines. For a long time, it has been recognized that the third vector component of the magnetic field plays an important role in the reconnection process;¹⁶ the southward interstellar magnetic field (IMF), which merges antiparallel to the Earth's northward dipole field, reconnects much faster at the meridian plane than the northward IMF. In the Versatile Toroidal Facility (VTF), an experimental study of reconnection has been carried out in the collisionless regime with the presence of a strong guide field. The collisionality of VTF was sufficiently low that electrons complete a full bounce trapped in the quadrupole field in the poloidal plane. The dynamics of the trapped electrons were studied and applied to the interpretation of the recent satellite data.⁵¹ But the effects of the strong guide field used in their experiment was not addressed explicitly.⁵¹

Recent experiments have shown that magnetic reconnection is influenced by the merging angle of the field lines.^{45–51} In an attempt to determine quantitatively the angle dependence of the reconnection speed, the magnitude of the external guide field was varied in TS-3 while the reconnecting field was kept roughly constant.⁴⁶ When the guide field was near zero (the reconnecting angle is near 180 degrees), the reconnection speed was maximized. When the reconnecting

angle was reduced as the guide field is increased, the reconnection speed decreased substantially, as shown in Fig. 9(a). In MRX it was also observed that the presence of the guide field changed the neutral sheet profile from the double “Y” shape to an “O” shape.^{47,48} A similar observation was first recorded by the UCLA group in the EMHD regime.⁶⁴

The formation and evolution of the plasma sheets was studied in the CS-3D⁵² device with variable guide field. With a guide field, a tilted neutral sheet was observed. The research was focused on the correlation between the structure of a plasma sheet and the topology of the initial 3D magnetic configuration. It was shown experimentally that the initial guide field is compressed in the neutral sheet and the compression decreases with increasing guide-field strength.

A 3D particle-in-cell simulation study was carried out by Pritchett⁵³ in an open geometry to investigate the effects of a guide field on collision-free magnetic reconnection. In his study, the quadrupole B_y pattern is replaced by an enhancement of the guide field component between the separatrices due to a paramagnetic effect. The enhanced parallel electric field and electron velocity are confined in a pair of separatrices, while the electron current density peaks on the other pair. With the presence of a strong guide field ($B_y \gg B_x$), the reconnection rate is reduced by factor of 2–3, which is consistent with the results from a 2D particle simulation by Horiuchi and Sato,⁵⁴ as shown in Fig. 9(b). These numerical results are also in qualitative agreement with the earlier experimental results for the local reconnection rate obtained in TS-3^{45,46} as shown in Fig. 9(a), and MRX⁴⁷, even though these experiments were carried out in relatively collisional plasmas. This agreement may suggest an answer to the question as to what basic physics mechanism is responsible for a slower rate in the guide reconnection case. Rather than Hall effects at the reconnection layer, the magnetic pressure of the guide field may be responsible for slowing down incoming magnetized plasma at the reconnection layer. Further study is needed to assess precisely the physics mechanisms of a guide field.

Another question can be raised as to why reconnection occurs so fast in tokamak sawtooth crashes, where the guide field is very strong. An answer to this may be that 3D MHD instabilities are destabilized to trigger a fast magnetic reconnection in a localized region, as will be described in Sec. IV.

E. Measurements of electromagnetic and electrostatic fluctuations

A substorm, an explosive release of magnetic energy, is considered to occur due to magnetic reconnection in the magnetotail. From many satellite observations, evidence of lower hybrid wave (LHW) fluctuations has been reported.^{55,56} During the substorm period, magnetic noise bursts with LHW frequencies were observed in the neutral sheet of the magnetotail. The Polar satellite recently observed in the magnetopause that electrostatic LHW fluctuations dominate at the edge of the neutral sheet while strong electromagnetic fluctuations exist at the center, as shown in Fig. 10(a), which shows a time sequence of detected wave amplitudes as the satellite passes through the neutral sheet.⁵⁶

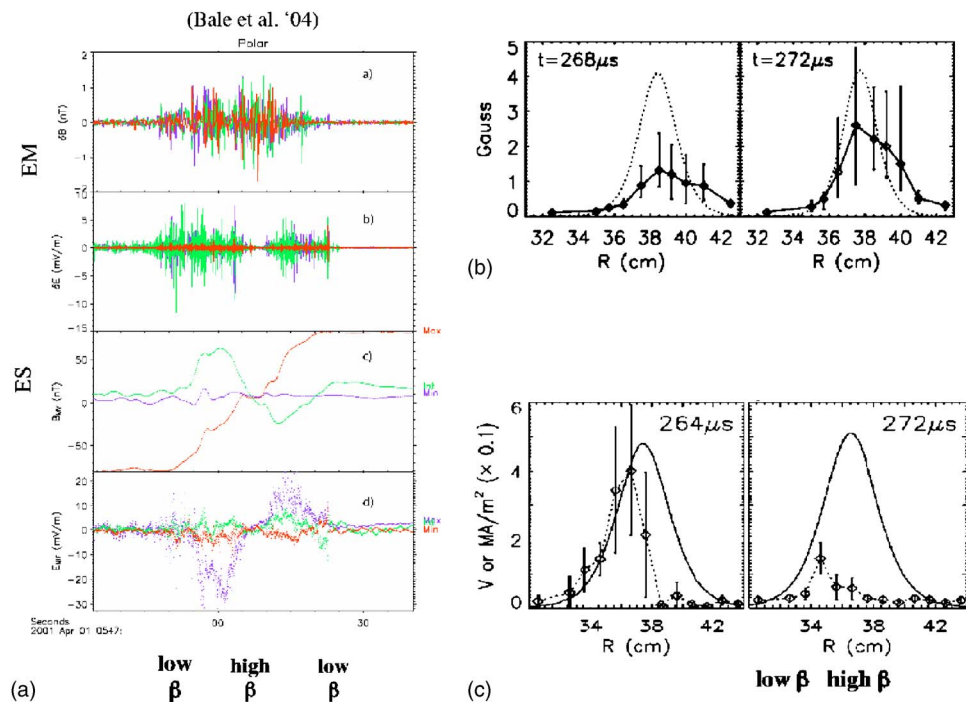


FIG. 10. (Color online) LHW fluctuation profiles: (a) magnetosphere data; [(b) and (c)] MRX data for electromagnetic (b) and electrostatic (c) wave amplitudes in two different times (Refs. 60 and 62).

To explain the observed fluctuations in the neutral sheets of the magnetosphere, many theoretical and numerical simulations have been carried out^{57–59} to reach a consensus that the lower hybrid drift instability can be excited in the periphery of the neutral sheet but should be stable in the central region of the neutral sheet due to its high beta values as well as by the grad B drift of electrons. A recent numerical analysis concludes that the LHDI excited at the periphery can modify the sheet current profile to a more peaked configuration that destabilizes electromagnetic LHWs. However, there is not yet a clear explanation of how they can induce fast reconnection or anomalous resistivity.

In searching for mechanisms responsible for the observed anomalous resistivity, electrostatic and electromagnetic high-frequency fluctuations have been investigated^{60–62} in MRX. In agreement with the theoretical prediction, it was found that electrostatic fluctuations peak at the low beta edge of the current sheet [Fig. 10(c)], while the electromagnetic fluctuations peak at the center of the current sheet [Fig. 10(b)]. The measured frequency spectra show that most fluctuations are in the lower hybrid frequency range, but it was found that the electrostatic fluctuations did not correlate with the observed enhanced resistivity or the fast reconnection rate. With the use of the hodogram probe, the observed EM waves have been identified as right-hand polarized Whistler waves propagating obliquely to the magnetic field. These fluctuations in the LHW frequency range appear in all three magnetic components when the current sheet forms, and persist as long as the reconnection proceeds. The dispersion relation of the wave was measured using the phase shift between two spatial points.⁶² The fluctuations have large amplitudes and appear consistently near the current sheet center with peak $\delta B/B_0 \sim 5\%$, where B_0 is the upstream reconnecting magnetic field. Importantly, a correlation has been found between the wave amplitudes and the fast reconnection rate

in the low-density regime. A linear local theory was formulated to explain destabilization of the observed EM waves. It was contemplated that a reactive coupling of Whistler wave in the moving electron frame and the magnetosonic mode in the resting ions generates unstable EM waves. However, the question remains as to how these EM waves contribute to fast reconnection in MRX. Recently, a quasilinear theory was developed to assess the effects of EM waves on the reconnection rate based on a local formulation.⁶³

In a reconnection experiment in the electron MHD (EMHD) regime, where electrons are magnetized and ions are not as their gyro-orbit exceeds the size of the plasma, ion acoustic waves were observed in the hot electron plasma ($T_e \gg T_i$) and they were attributed to the observed anomalous resistivity.⁶⁴

IV. INVESTIGATION OF GLOBAL RECONNECTION PHENOMENA

Magnetic energy in a low- β plasma is stored in a force-free magnetic equilibrium configuration. When an external force is applied to the plasma, the magnetic configuration gradually changes to a new equilibrium while plasma parameters slowly adjust. When the new state is unstable, the plasma rapidly reorganizes itself to a new MHD equilibrium state, which forms current sheets and drives magnetic reconnection. This paradigm for global magnetic reconnection can be applied to most magnetic self-organization in laboratory and space plasmas.

The study of global reconnection phenomena in the laboratory can contribute to the understanding of the Sun's coronal behavior through overall understanding of magnetic relaxation phenomena or reconnection. Although the geometrical analogy cannot be applied straightforwardly, quantitative analysis of laboratory experimental results may

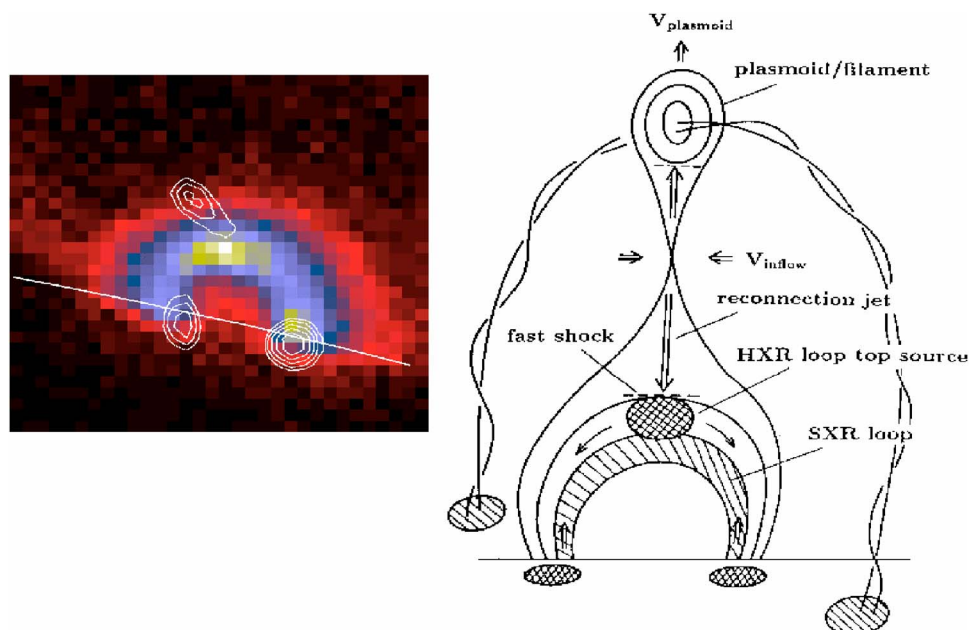


FIG. 11. (Color online) A hard-x-ray image from the top of an arcade (Ref. 8) and a CME model (Ref. 68).

be able to help interpret the solar observation data of a specific scope or the relaxation phenomena of the magnetosphere. Magnetic reconnection is a key element of relaxation of toroidal pinch plasmas such as the tokamak,⁶⁵ RFP (reversed field pinch),⁶⁶ and spheromak.⁶⁷ Significant effort has been devoted to studies of sawtooth relaxation of these current-carrying plasmas. In this section, we will carefully examine the results of toroidal fusion plasmas, keeping a focus on our common paradigm, namely, “as magnetic energy is stored in a force-free magnetic equilibrium configuration via slow adjustment of an external parameter, the plasma often suddenly reorganizes itself to a new MHD equilibrium state, which forms current sheets and drives magnetic reconnection.”

A. Reconnection in solar flares

Solar flares, whose topologies can be seen to change within a time scale of minutes through soft-X-ray pictures, are apparently the most illuminating examples of global topology change of a plasma indicating global magnetic reconnection phenomena. However, the change of magnetic field topology is hard to verify, because magnetic field profiles can be measured only at the photo surface from Zeeman spectroscopy. By using MHD codes and assuming little current in the plasma, some attempts have made limited success in deducing the evolution of coronal magnetic field profiles by applying MHD codes to measured surface field distributions.

Many theories and numerical simulations have been performed in order to determine detailed mechanisms of solar flare evolution. Some theoretical work has focused on two-dimensional models of the evolution of force-free magnetic arcades, in which field line footpoints are advected by flows in the solar photosphere.^{68–72} For example, a 2D flux-rope model has been proposed by Forbes and Priest to describe the eruption process of solar flares by ideal MHD. It demonstrated that the equilibrium of a flux rope jumps from one state to the other through the formation of a current sheet or

reconnection layer in the solar atmosphere. Some recent works address 3D effects. During magnetic reconnection, conversion of magnetic energy should occur in the solar corona, where much higher plasma temperatures than that of the photosphere is routinely observed.

Since the launches of recent satellites such as YOKOH, SOHO, and TRACE, a wealth of observational evidence for magnetic reconnection has been obtained. For example, cusp-shaped flare loops consistent with the classical reconnection models were observed. By studying profiles of hard-X-ray emissions, evidence of particle acceleration has been found at the top of soft-X-ray flares concomitantly with the appearance of impulsive flares or CMEs. Masuda *et al.* postulated that magnetic reconnection occurs as predicted by the classical model for long-duration-event (LDE) flares and that high speed jets produced by reconnection intersect with the top of the reconnected flare loop to produce a hot region represented by a strong hard-X-ray emission. Based on this observation, Shibata proposed a model by modifying the earlier flare models, as shown in Fig. 11(b). Recently, Yokoyama *et al.* estimated the reconnection speed⁷⁰ based on the evolution of soft-X-ray pictures from Yohkoh and concluded that the reconnection speed is in the relatively wide range of $0.001\text{--}0.05 V_A$. More recently launched satellites, SOHO and TRACE, generated more data useful for understanding reconnection in the Sun. Two new satellites, Solar B (Hinode) and STEREO, were successfully launched in the fall of 2006, and a new set of data will be available to elucidate detailed features of magnetic reconnection in the Sun’s surface

Recently, the role of helicity has been evaluated in the evolution of solar flares. It was observed⁷² that there is a preference in the direction of twist (which is closely related to the sign of helicity) in solar filaments depending on their hemisphere. For example, reverse-S-shaped filaments preferentially appear in the northern hemisphere, while S-shaped filaments preferentially appear in the southern hemisphere.

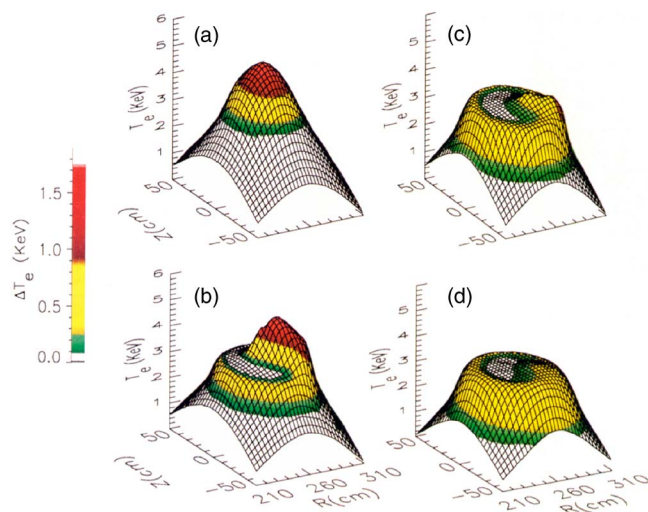


FIG. 12. (Color online) Electron cyclotron emission (ECE) shows evolution of $T_e(r)$ profiles during the crash phase of tokamak sawtooth relaxation. Here transfer, $\Delta T_e(r)$, during this period is color-coded. The time separation between each figure is 120 μs (Ref. 74).

Similarly, the current helicity ($\mathbf{j} \cdot \mathbf{B}$) measured by vector magnetographs, which is closely related to magnetic helicity, shows a corresponding preference in sign in the two hemispheres. When two such twisted filaments interact with each other, the observed reconnecting rate depends on the helicity of each filament.⁷² A helicity conservation principle was verified in RFP and spheromak plasmas⁴ as well as plasma-merging experiments. A new numerical analysis was carried out to understand the evolution of solar flares based on this concept.⁷¹ Plasma-merging with a variety of combinations of helicity was carried out in laboratory experiments⁴⁶ and helicity conservation was qualitatively confirmed.

B. Magnetic reconnection during a tokamak sawtooth crash

A tokamak sawtooth oscillation^{65,73} is characterized by a periodic repetition of peaking and sudden flattening (or crash) of the electron temperature T_e profile. The crash phase shown in Fig. 12 represents a typical relaxation process that manifests important physics mechanisms of magnetic reconnection,⁷⁴ since fast breaking of field lines and topological rearrangement occurs during a very short period ($\Delta t \sim 100 \mu\text{s}$). The sequence of a sawtooth oscillation proceeds as follows: The peaked T_e profile in a tokamak discharge often leads to a more highly peaked current profile with central q being reduced to less than unity, where q denotes the safety factor, or the inverse of rotational transform that depicts the pitch of field lines.⁶⁵ Due to this current profile, a helical MHD instability develops near the $q=1$ flux surface and this instability can induce driven magnetic reconnection. Kadomtsev proposed that this reconnection event (crash) should make the central q rise to unity, and similar cyclic evolutions would be repeated.

The electron cyclotron emission (ECE) radiation spectrum, which determines the T_e profile, can provide the configuration of flux surfaces on which T_e can be assumed constant. During the crash, a fast heat transfer was observed

from the inside to the outside of the $q=1$ surface. The T_e profile inside the inversion radius becomes completely flat after the crash, which is consistent with Kadomtsev's prediction, as seen in Figs. 12(b) and 12(c). This fast heat flow was attributed to magnetic reconnection, which was verified by a measurable change of q in the crash phase by the motional Stark effect (MSE) diagnostic system. The measured q profiles indicated that the central q value increased by 5–10% typically from 0.7 to 0.75 during the sawtooth crash phase but did not relax to unity, even while the pressure gradient diminished inside the $q=1$ region. Throughout the sawtooth cycle, the q value at the center (magnetic axis), q_0 , was kept below unity. The observations raised an important question as to why the magnetic field lines inside the $q=1$ region did not form a flat $q \sim 1$ inner region after the crash as suggested by Kadomtsev, while the temperature gradient diminishes to zero as predicted for full reconnection. A simultaneous analysis of $T_e(r, \theta)$ and $q(R)$ profile evolutions⁷⁴ leads to a heuristic model. In this model, a 3D kink mode develops and displaces the pressure contours on an ideal MHD time scale with a helical ($m=1$, $n=1$ poloidal and toroidal mode numbers) structure, thus inducing a forced reconnection in a localized region in both toroidal and poloidal directions. A rapid efflux of thermal energy occurs through the X-point region along newly connected field lines due to the stochasticity of tokamak. This idea was later supported by Bhattacharjee *et al.* by numerical simulation. The precipitous drop of the pressure gradient, which occurs within a short period of $100\text{--}200 \mu\text{s} \ll t_{\text{Sweet-Parker}}$,^{1,17,18} removes the free energy to drive the kink instability, inhibiting full reconnection.

Most recently, Park *et al.*^{77,78} measured 2D profiles of the electron temperature of the TEXTOR tokamak using sophisticated 2D arrays of electron cyclotron emission spectroscopy. It was found that magnetic reconnection occurs very fast, $< 100 \mu\text{s}$, much shorter time than the Sweet-Parker time, and this confirmed that reconnection occurs in a localized region in both toroidal and poloidal directions in agreement with ballooning-based models.^{74–76} However, they found the reconnection region to be arbitrarily distributed both on the high and low toroidal field side of the tokamak, contrary to the ballooning-based models, which predict reconnection occurs predominantly on the lower field side.

The recent extensive study of sawtooth relaxation in tokamaks reveals the following:

- (1) Magnetic reconnection is often driven by an ideal MHD instability generated in a gradual change of tokamak equilibrium and the reconnection time is much faster than the classical value.
- (2) Heat diffusion transport can occur at a much faster rate than the magnetic reconnection rate and influences the features of magnetic self-organization.

C. Magnetic reconnection during a RFP sawtooth relaxation

In the RFP, magnetic reconnection occurs through a self-organization process of a toroidally confined plasma, which can be both continuous and impulsive. Magnetic energy is stored in a force-free magnetic equilibrium configuration via

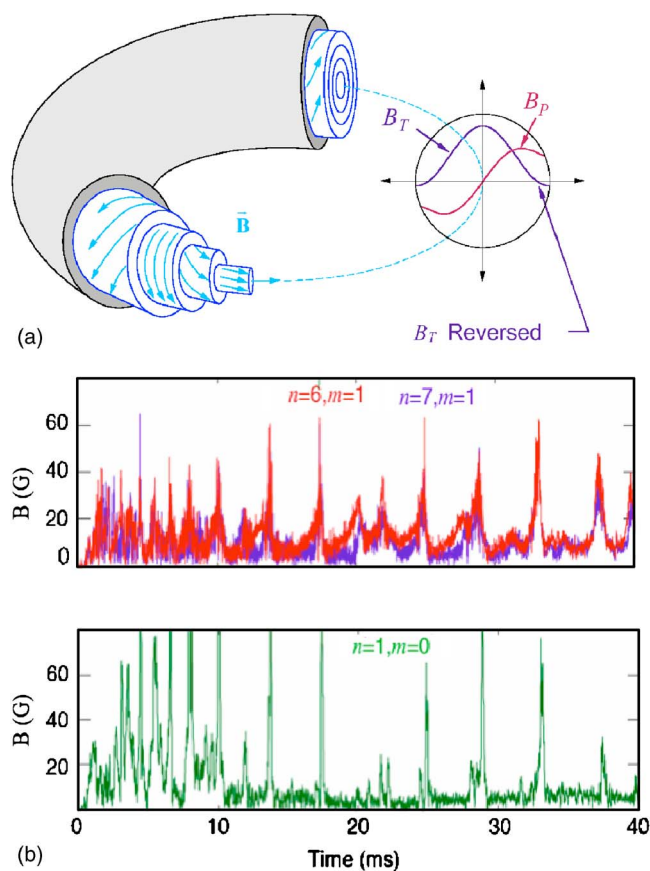


FIG. 13. (Color online) (a) Schematic of MST plasma configuration showing magnetic field lines, strongly sheared. Reconnection can occur at multiple surfaces, such as those indicated in the cutaway view of the toroidal plasma. The radial dependence of the poloidal and toroidal magnetic fields is plotted. (b) Reconnecting magnetic field vs time for spontaneous reconnection (top) and driven reconnection (bottom). The toroidal and poloidal mode numbers (m, n) of the different reconnection structures are indicated. The sudden, explosive nature of the reconnection is apparent.

a slow adjustment to external driving force. With sawtooth events, plasma suddenly reorganizes itself to a new MHD equilibrium state, which forms current sheets and drives magnetic reconnection, the common theme of this section. In this device, the role of local reconnection in the global relaxation phenomena has been studied. The plasma contains a sheared magnetic field [Fig. 13(a)] because the equilibrium magnetic field pitch changes its direction from the center (primarily toroidal) to the edge of the plasma (poloidal). Since the field lines are sheared, reconnection occurs at multiple radii in the torus, with each radial location corresponding to a rational surface in which the safety factor is defined by m/n . Often the multiple reconnections occur suddenly and simultaneously, leading to a sudden global rearrangement of the magnetic field. It was found that the global helicity tends to be conserved while the total magnetic energy is dissipated,⁷⁹ in agreement with the Taylor principle.

As mentioned in Sec. III, Hall reconnection effects were measured in the Madison Symmetric Torus (MST) device and were shown to be important. A linear two-fluid tearing instability calculation has been performed for the relevant experimental configuration.⁴⁰ The theory predicts that the

Hall term dominates the single fluid term in Ohm's law close to the reconnection layer, and is confirmed by measurements.

In a RFP, spontaneous reconnection occurs in the plasma core and, under some conditions, in the cool edge. In addition, two unstable core tearing modes can nonlinearly couple to produce a driven reconnection at a third location in the plasma edge region, as seen in Fig. 13(b). This nonlinearly driven reconnection can equivalently be viewed as resulting from the flows produced by the combined effect of two unstable modes. A similar phenomenon can occur in active solar arcades flares where a spontaneous reconnection in the internal core can drive reconnection in the outer layer. Based on this hypothesis, a new scenario of solar flare eruption has been proposed.⁶⁹ It will be particularly interesting to compare the relationship and time sequence between the spatial structures of spontaneous and driven reconnection regions of RFP plasmas with those of solar flare eruptions. It is also observed that the ion temperature increases significantly during this RFP relaxation event.⁸⁰ The exact mechanisms for this anomalous heating are not yet known.

D. Study of intermittent relaxation in a dedicated laboratory device

In the closed magnetic surface configuration implemented in the Versatile Toroidal Facility (VTF), intermittent reconnection events have recently been observed; in some discharges the reconnection dynamics is slow at first, then is followed by a burst of fast reconnection.⁸¹ As the X-line region becomes more and more elongated, it reaches a critical level of magnetic stress after which the plasma current decreases rapidly and the reconnection rate jumps to a large value. The details of the intermittent dynamics are illustrated in Fig. 14. The bottom row of subfigures shows the measured contours of $-\partial\Psi/\partial t$ during a 24 μs period centered on the reconnection event. The dashed lines are the magnetic field lines, which coincide with contours of constant Ψ (obtained by integrating $\partial\Psi/\partial t$ from the beginning of the discharge). In the first two time slices, the reconnection region is becoming increasingly stretched. Then, for a time interval of about 15 μs , the reconnection rate jumps well above 10 V/m. In this time interval, the highlighted set of field lines merge, reconnect, and drift apart while the magnetic stress in the system is greatly reduced. In the top row of Fig. 14, the measured field lines are superimposed on contours of measured plasma density. During the reconnection event, it is seen how the central density is ejected downwards at a velocity consistent with the motion of the highlighted magnetic field lines. A more detailed analysis shows that the plasma moves downwards at about 20 km/s, corresponding to a significant energization of the argon ions. In fact, energy balance calculations show that nearly all the magnetic energy is transferred to kinetic energy in the near Alfvénic plasma outflow.

V. SUMMARY AND FUTURE RESEARCH ISSUES

In the past two decades, important findings and discoveries have been made on the fundamental physics of magnetic reconnection.

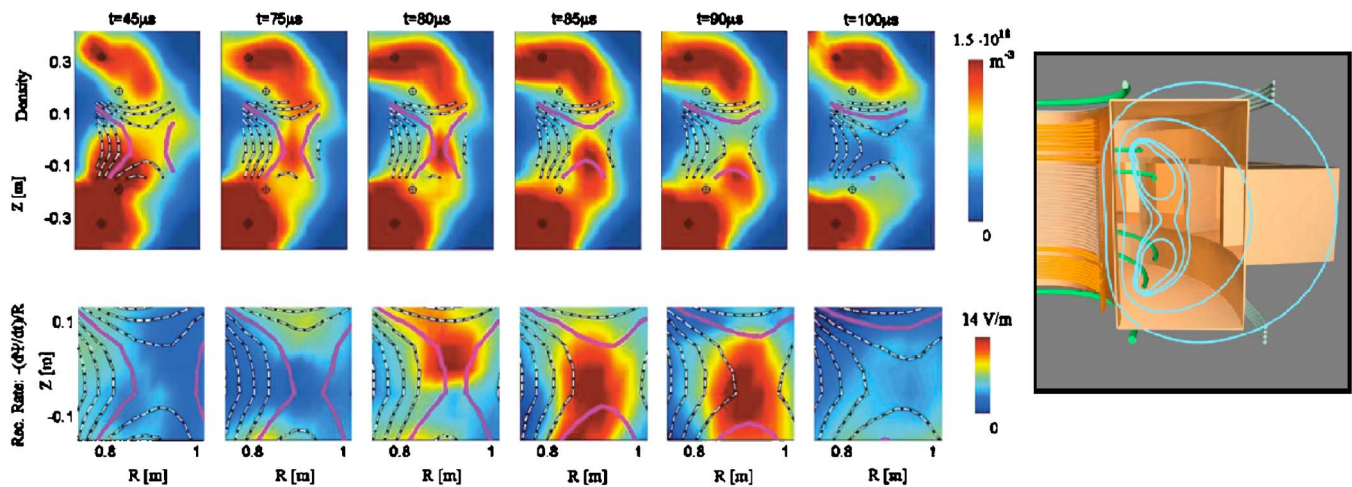


FIG. 14. (Color online) (Right) Poloidal cross section of the VTF. The solid blue lines show the poloidal field geometry. (Left) Measured contours of the plasma density and the reconnection rate, $-\partial\Psi/\partial t$. The measurements were obtained in a $5 \mu\text{s}$ time interval centered about a spontaneous reconnection study of the neutral sheath (Ref. 81).

With regard to the local reconnection physics, significant progress has been made with the following findings:

- (1) In laboratory experiments, the reconnection rate is found to increase rapidly as the ratio of the electron mean free path to the scale length increases.
- (2) The verification of Hall-MHD effects was made in numerical simulations and in both laboratory and space plasmas.
- (3) It was found in a laboratory experiment that the shape of the reconnection layer changes drastically as collisionality of plasma is varied. In a highly collisional plasma, a rectangular shape Sweet-Parker reconnection layer was identified. In the collision-free regime, the shape of the reconnection layer changes to a Petschek-like double edge with a much larger reconnection rate.
- (4) It was found both in experiments and numerical simulations that the reconnection rate depends on merging angle of field lines (effect of guide field), with the guide field slowing down the reconnection rate.
- (5) Electrostatic and electromagnetic fluctuations are observed in the neutral sheets of both laboratory and space plasmas, with notable similarities in their characteristics and their theoretical interpretation. In a laboratory experiment, a correlation was found between the reconnection rate and the amplitude of EM waves.

In the area of global reconnection, major progress has been made in documenting key features of magnetic self-organization with the following findings:

- (6) In solar flares, reconnection sites were identified with hard-x-ray emissions near the top of solar flare arcades during CMEs and coronal eruptions.
- (7) In tokamaks, magnetic reconnection is often driven by an ideal MHD instability generated in a gradual change of tokamak equilibrium, and the reconnection time is much shorter than the classical value.
- (8) In RFPs, anomalous ion heating and momentum transport are documented during sawtooth relaxation events.

- (9) Strong ion acceleration and heating are measured in spheromak merging experiments.

In the past decade, significant effort has been devoted to finding essential dynamics of reconnection in the two-fluid or the collisionless regime. It is now very important to know under what conditions the two-fluid dynamics become important and to identify criteria for the transition from the one-fluid to the two-fluid regime.

Recent MRX data suggest that this happens when the scale size of the reconnection layer [the smaller of δ (thickness) or L (length), namely δ] becomes comparable to the electrons' mean free path as suggested in Fig. 5(a) in Sec. III. Recently, more extensive study has been carried out with regard to how the reconnection rate depends on collisionality. In the two-fluid regime, the sheet thickness is generally determined by the ion skin depth, $\delta_i = c/\omega_{pi}$. On the other hand, in the one-fluid collisional MHD regime, the sheet thickness is determined by the Sweet-Parker width, $L/S^{1/2}$. An important parameter should then be the ratio of the ion skin depth to the Sweet-Parker layer thickness, δ_{SP} . Taking the ratio of the ion skin depth to the Sweet-Parker width, we find the relationship is translated into the square root of the ratio of the electron mean free path to the system size (length),

$$\frac{\delta_i}{\delta_{SP}} = \frac{\frac{c}{\omega_{pi}}}{L \frac{c}{\omega_{pe}} \sqrt{\left(\frac{2v_{the}}{\lambda_{mfp}} \frac{1}{V_A L}\right)}} \quad (6a)$$

or

$$= 4.5 \left(\frac{\lambda_{mfp}}{L}\right)^{1/2} \left(\frac{m_i}{m_{iH}}\right)^{1/4}, \quad (6b)$$

where m_i and m_{iH} are mass number for plasma ions and protons, and we have assumed $T_e \sim T_i$ and $\eta_{\perp} = 2\eta_{\parallel}$, $V_A \sim v_{thi}$ ($\beta \sim 1$) and $m_{iH}/m_e \sim 1800$.

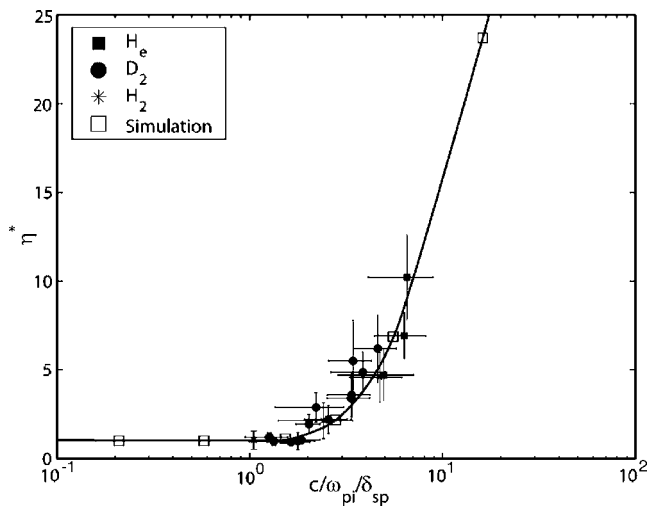


FIG. 15. MRX scaling, Effective resistivity $\eta^* = (E/j)$ normalized by the Spitzer value η_{SP} vs the ratio of the ion skin depth to the Sweet-Parker width is compared with numerical calculation of the contributions of Hall-MHD effects to the reconnection electric field. The simulations were based on a 2D two-fluid code (Refs. 28 and 39).

In MRX, the classical rate of reconnection with the Spitzer resistivity is obtained³⁸ when the collisional resistivity is large enough to satisfy $c/\omega_{pi} < \delta_{SP}$. When the ion skin depth becomes larger than δ_{SP} , the reconnection layer thickness is expressed by $0.4 c/\omega_{pi}$ and the reconnection rate is larger than the classical reconnection rate determined by Spitzer resistivity. Figure 15 presents an MRX scaling for effective resistivity $\eta^* = \eta_{eff}/\eta_{SP}$ ($\eta_{eff} = E/j$) normalized by the Spitzer value η_{SP} in the center of the reconnection region in comparison with a scaling obtained in a recent Hall-MHD numerical simulation using a two-fluid MHD code. The horizontal axis represents the ratio of the ion skin depth normalized by the classical Sweet-Parker width ($\delta_{SP} = L/\sqrt{S_{eff}}$), where the system scale, L , was set to be 20 cm. This figure exhibits an important criterion for the two-fluid effects to become important, namely the reconnection resistivity (or reconnection speed) takes off from the classical Spitzer value (or the Sweet-Parker reconnection rate) when the ion skin depth, δ_i , becomes larger than the Sweet-Parker width, δ_{SP} , by a factor of 2. The apparent agreement of the MRX scaling with two-fluid Hall MHD code indicates that the measured anomalous resistivity is primarily due to the laminar Hall effect, when the Spitzer resistivity is not large enough to balance the large reconnecting electric field in fast magnetic reconnection. In the numerical simulation,³⁹ it was seen that the reconnection electric field is primarily generated by the laminar Hall effect, namely $j_{Hall} \times B$ term, and this is consistent with the MRX data shown in Fig. 15.

However, this does not exclude fluctuations for active participation in fast reconnection, since the electromagnetic fluctuations appear when Hall effects become dominant. Since the magnitude of the laminar Hall effect peaks outside of the X line goes to zero at the X line, additional effects, such as anomalous resistivity caused by turbulence, are needed to support reconnection electric field around the X line and separatrixes.²⁸ It can thus be viewed that both

mechanisms, one based on the laminar Hall effect and the other based on turbulence, can be responsible for fast reconnection.

To find out the true cause of magnetic reconnection, another important step is to clarify the interrelationships between laminar Hall dynamics and magnetic fluctuations at the neutral sheet. At the moment, there is no clear consensus with regard to how the observed waves are excited and how they affect reconnection rate or dissipation.

It is planned to extend this scaling study of reconnection rate to the cases of guide-field reconnection. It is also important to develop the theory of reconnection in weakly ionized systems, such as the interstellar medium.⁸² There are preliminary indications that the Hall regime is pushed to larger length scales because ion-neutral friction increases the effective ion inertia, thus making the two-fluid regime wider.

To analyze global magnetic self-organization processes, it is important to understand how large-scale systems generate the local reconnection structures, through the formation of current sheets, either arising spontaneously or forced by boundary conditions. Progress has been made in toroidal plasmas, by documenting the processes in which plasma reorganizes itself suddenly to a new MHD equilibrium state forming current sheets and driving magnetic reconnection. Actual reconnection phenomena are often influenced by boundary conditions. It is necessary to determine under what conditions and how they come into play.

As magnetic energy is converted to particle energy, it is essential to determine mechanisms of particle heating and acceleration during reconnection by exploring the relationship between anomalous particle acceleration and heating and reconnection events in both laboratory and astrophysical plasmas. Another important question is why T_i is generally higher than T_e after reconnection. Magnetic reconnection and anomalous ion heating are observed to be closely associated in both laboratory and astrophysical plasmas.

One of the most important issues in both laboratory and astrophysical plasmas is to find the relationship between global phenomena such as magnetic self-organization, which occurs in very wide range of scales, and local scale physics of magnetic reconnection. In this context, it is essential to find out the relationship between reconnection and magnetic dynamos. Is reconnection always needed to have dynamos? To answer this, we have to investigate how the local reconnection process contributes to global dynamo activities through flux conversion process or other means.

Thanks to the advances in laboratory plasma experiments and the surge of space astrophysical data from new satellites, we expect further advances in this field to gain a new understanding of the key mechanisms of the interplay between the magnetic field and plasmas.

ACKNOWLEDGMENTS

The author appreciates many productive discussions with Dr. R. Kulsrud, Dr. H. Ji, Dr. Y. Ren, Dr. A. Bhattacharjee, Dr. J. Drake, Dr. E. Zweibel, and the members of "Physics Frontier Center for Magnetic Self-Organization in Laboratory and Astrophysical Plasmas," which is jointly

supported by the National Science Foundation and the Department of Energy. The author is also thankful for the careful reading of this manuscript by Craig Jacobson.

- ¹E. N. Parker, *Cosmical Magnetic Fields* (Clarendon, Oxford, 1979); *Astrophys. J.* **180**, 247 (1973).
- ²E. Priest and T. Forbes, *Magnetic Reconnection* (Cambridge University Press, Cambridge, UK, 2000).
- ³D. Biskamp, *Magnetic Reconnection in Plasmas* (Cambridge University Press, Cambridge, UK, 2000).
- ⁴J. B. Taylor, *Rev. Mod. Phys.* **58**, 741 (1986).
- ⁵R. M. Kulsrud, *Phys. Plasmas* **5**, 1599 (1998); **2**, 1735 (1995).
- ⁶M. Yamada, *J. Geophys. Res.* **104**, 14529 (1999).
- ⁷S. Tsuneta, *Astrophys. J.* **456**, 840 (1996); *Astrophys. J. Lett.* **456**, L63 (1996).
- ⁸S. Masuda, T. Kosugi, H. Hara *et al.*, *Nature* **371**, 495 (1994).
- ⁹J. L. Kohl, G. Noci, E. Antonucci *et al.*, *Sol. Phys.* **175**, 613 (1997).
- ¹⁰L. Golu, J. Bookbinder, E. Deluca *et al.*, *Phys. Plasmas* **6**, 2205 (1999).
- ¹¹R. P. Lin, S. Krucker, G. L. Hurford *et al.*, *Astrophys. J. Lett.* **595**, L69 (2003).
- ¹²J. W. Dungey, "Origin of the concept of reconnection and its application to the magnetopause," in *Physics of the Magnetopause*, Geophysical Monograph No. 90, edited by P. Song, B. O. Sonnerup, and M. F. Thomsen (American Geophysical Union, Washington, D.C., 1995), pp. 81–98.
- ¹³V. M. Vasyliunas, *Rev. Geophys. Space Phys.* **13**, 303 (1975).
- ¹⁴G. Kivelson and C. T. Russell, *Introduction to Space Physics* (Cambridge University Press, London, 1995); C. T. Russell and R. C. Elphic, *Geophys. Res. Lett.* **6**, 33 (1979).
- ¹⁵C. L. Litwin, E. R. Brown, and R. Rosner, *Astrophys. J.* **553**, 788 (2001).
- ¹⁶M. Yamada, *Earth, Planets Space* **53**, 509 (2001).
- ¹⁷P. A. Sweet, "The neutral point theory of solar flares," in *Electromagnetic Phenomena in Cosmical Physics*, edited by B. Lehnert (Cambridge University Press, New York, 1958), p. 123.
- ¹⁸E. N. Parker, *J. Geophys. Res.* **62**, 509 (1957).
- ¹⁹H. E. Petschek, "Magnetic field annihilation," *NASA Spec. Pub. SP-50*, 425 (1964).
- ²⁰J. F. Drake, *Nature* **410**, 557 (2001).
- ²¹H. Horiuchi and T. Sato, *Phys. Plasmas* **6**, 4565 (1999).
- ²²J. Birn, J. F. Drake, M. Shay *et al.*, *J. Geophys. Res.* **106**, 3715 (2001).
- ²³M. A. Shay and J. F. Drake, *Geophys. Res. Lett.* **25**, 3759 (1998).
- ²⁴P. L. Pritchett, *J. Geophys. Res.* **106**, 25961 (2001).
- ²⁵M. Yamada, H. Ji, S. Hsu *et al.*, *Phys. Plasmas* **7**, 1781 (2000).
- ²⁶F. Mozer, S. Bale, and T. Phan, *Phys. Rev. Lett.* **89**, 015002 (2002).
- ²⁷Y. Ren, M. Yamada, H. Ji *et al.*, *Phys. Rev. Lett.* **95**, 055003 (2005).
- ²⁸M. Yamada, Y. Ren, H. Ji *et al.*, *Phys. Plasmas* **13**, 052119 (2006).
- ²⁹M. Brown, C. D. Cothran, and J. Fung, *Phys. Plasmas* **13**, 056503 (2006).
- ³⁰J. W. Dungey, *Philos. Mag.* **44**, 725 (1953).
- ³¹H. P. Furth, J. Killeen, and M. N. Rosenbluth, *Phys. Fluids* **16**, 1054 (1963).
- ³²H. Ji, M. Yamada, S. Hsu, and R. Kulsrud, *Phys. Rev. Lett.* **80**, 3256 (1998).
- ³³H. Ji, M. Yamada, S. Hsu *et al.*, *Phys. Plasmas* **6**, 1743 (1999).
- ³⁴T. Sato and T. Hayashi, *Phys. Fluids* **22**, 1189 (1979).
- ³⁵M. Ugai and T. Tsuda, *J. Plasma Phys.* **17**, 337 (1977).
- ³⁶D. Uzdensky and R. M. Kulsrud, *Phys. Plasmas* **7**, 4018 (2000).
- ³⁷D. Uzdensky and R. Kulsrud, *Phys. Plasmas* **13**, 062305 (2006).
- ³⁸F. Trintchouk, M. Yamada, H. Ji, R. M. Kulsrud, and T. A. Carter, *Phys. Plasmas* **10**, 319 (2003).
- ³⁹J. Breslau and S. Jardin, *Phys. Plasmas* **10**, 1291 (2003).
- ⁴⁰W. X. Ding, D. L. Brower, D. Craig *et al.*, *Phys. Rev. Lett.* **93**, 045002 (2004).
- ⁴¹F. S. Mozer, *J. Geophys. Res.* **110**, A12222 (2005).
- ⁴²Z. W. Ma and A. Bhattacharjee, *Geophys. Res. Lett.* **23**, 167 (1996).
- ⁴³A. Bhattacharjee, *Annu. Rev. Astron. Astrophys.* **42**, 365 (2001).
- ⁴⁴P. A. Cassak, M. A. Shay, and J. F. Drake, *Phys. Rev. Lett.* **95**, 235002 (2005).
- ⁴⁵M. Yamada, Y. Ono, A. Hayakawa, and M. Katsurai, *Phys. Rev. Lett.* **65**, 721 (1990).
- ⁴⁶Y. Ono, A. Morita, M. Katsurai, and M. Yamada, *Phys. Fluids B* **5**, 3691 (1993).
- ⁴⁷M. Yamada, H. Ji, S. Hsu *et al.*, *Phys. Plasmas* **4**, 1936 (1997).
- ⁴⁸M. Yamada, H. Ji, S. Hsu *et al.*, *Phys. Rev. Lett.* **78**, 3117 (1997).
- ⁴⁹M. Brown, *Phys. Plasmas* **6**, 1717 (1999).
- ⁵⁰J. Egedal, W. Fox, M. Porkolab *et al.*, *Phys. Plasmas* **11**, 2844 (2004).
- ⁵¹J. Egedal, M. Oieroset, W. Fox, and R. Lin, *Phys. Rev. Lett.* **94**, 025006 (2005).
- ⁵²A. G. Frank, S. Y. Bogdanov, V. S. Markov *et al.*, *Phys. Plasmas* **12**, 052316 (2005).
- ⁵³P. L. Pritchett and F. V. Coroniti, *J. Geophys. Res.* **109**, A01220 (2004).
- ⁵⁴R. Horiuchi and T. Sato, *Phys. Plasmas* **4**, 277 (1997).
- ⁵⁵I. Shinohara, T. Nagai, M. Fujimoto *et al.*, *J. Geophys. Res.* **103**, 20365 (1998).
- ⁵⁶S. Bale, F. S. Mozer, and T. Phan, *Geophys. Res. Lett.* **29**, 2180 (2002).
- ⁵⁷G. Lapenta and J. Brackbill, *Phys. Plasmas* **9**, 1544 (2002).
- ⁵⁸W. Daughton, G. Lapenta, and P. Ricci, *Phys. Rev. Lett.* **93**, 105004 (2004).
- ⁵⁹R. Horiuchi and T. Sato, *Phys. Plasmas* **6**, 4565 (1999).
- ⁶⁰T. A. Carter, H. Ji, S. Hsu *et al.*, *Phys. Rev. Lett.* **88**, 015001 (2002).
- ⁶¹T. Carter, M. Yamada, H. Ji *et al.*, *Phys. Plasmas* **9**, 3272 (2002).
- ⁶²H. Ji, S. Terry, M. Yamada *et al.*, *Phys. Rev. Lett.* **92**, 115001 (2004).
- ⁶³R. Kulsrud, H. Ji, W. Fox, and M. Yamada, *Phys. Plasmas* **12**, 082301 (2005).
- ⁶⁴R. L. Stenzel and W. Gekelman, *J. Geophys. Res.* **86**, 649 (1981); W. Gekelman, R. L. Stenzel, and N. Wild, *ibid.* **87**, 101 (1982).
- ⁶⁵J. Wesson, *Tokamak* (Clarendon, Oxford, 1987).
- ⁶⁶J. B. Taylor, *Phys. Rev. Lett.* **33**, 1139 (1974).
- ⁶⁷P. Bellan, *Spheromaks* (Imperial College Press, London, 2000).
- ⁶⁸K. Shibata, *Astrophys. J., Lett. Ed.* **33**, 1139 (1974).
- ⁶⁹K. Kusano, T. Maeshiro, T. Yokohama *et al.*, *Astrophys. J.* **610**, 537 (2004).
- ⁷⁰T. Yokoyama, K. Akita, T. Morimoto *et al.*, *IAU SYMPOSIA* **203**, 318 (2001).
- ⁷¹A. K. Antiochos, C. R. DeVore, and J. A. Klimchuk, *Astrophys. J.* **510**, 485 (1999).
- ⁷²D. M. Rust and A. Kumer, *Sol. Phys.* **155**, 69 (1994); A. A. Pevtsov, R. C. Canfield, and T. R. McClymont, *Astrophys. J. Lett.* **425**, L117 (1994).
- ⁷³B. B. Kadomtsev, *Sov. J. Plasma Phys.* **1**, 389 (1975).
- ⁷⁴M. Yamada, F. Levinton, N. Pomphrey *et al.*, *Phys. Plasmas* **1**, 3269 (1994).
- ⁷⁵F. Levinton, S. Batha, M. Yamada, and M. Zarnstorff, *Phys. Fluids B* **5**, 2554 (1993).
- ⁷⁶W. Park, F. Fredrickson, A. Janos *et al.*, *Phys. Rev. Lett.* **75**, 1763 (1995).
- ⁷⁷H. Park, N. C. Luhman, A. J. H. Donne *et al.*, *Phys. Rev. Lett.* **96**, 195003 (2006).
- ⁷⁸H. Park, A. J. H. Donne, N. C. Luhman *et al.*, *Phys. Rev. Lett.* **96**, 195004 (2006).
- ⁷⁹H. Ji, S. C. Prager, A. F. Almagri *et al.*, *Phys. Plasmas* **3**, 1935 (1996).
- ⁸⁰G. Fiksel, A. F. Almagri, J. K. Anderson *et al.*, "Confinement of high energy and high temperature ion in the MST reversed field pinch," *Nucl. Fusion* (to be published).
- ⁸¹J. Egedal, W. Fox, N. Katz, M. Porkolab, K. Reim, and E. Zhang, *Phys. Rev. Lett.* **98**, 015003 (2007).
- ⁸²E. G. Zweibel, *Astrophys. J.* **340**, 550 (1989).